Available online at www.sciencedirect.com

ScienceDirect

www.elsevier.com/locate/jes

JES JOURNAL OF ENVIRONMENTAL SCIENCES www.jesc.ac.cn

Spatiotemporal trends of $PM_{2.5}$ and its major chemical components at urban sites in Canada

Huanbo Wang[1,**], *Leiming Zhang*[2,*], *Irene Cheng*[2], *Xiaohong Yao*[3], *Ewa Dabek-Zlotorzynska*[4]

[1] *School of Environment and Resource, Southwest University of Science and Technology, Mianyang 621010, China*
[2] *Air Quality Research Division, Science and Technology Branch, Environment and Climate Change Canada, Toronto, Canada*
[3] *Lab of Marine Environmental Science and Ecology, Ministry of Education, Ocean University of China, Qingdao 266100, China*
[4] *Air Quality Research Division, Science and Technology Branch, Environment and Climate Change Canada, Ottawa, Canada*

ARTICLE INFO

Article history:
Received 8 July 2020
Revised 29 September 2020
Accepted 29 September 2020
Available online 24 October 2020

Keywords:
Fine particulate matter
Aerosol chemical composition
Monitoring network

ABSTRACT

To evaluate the effectiveness of emission control regulations designed for reducing air pollution, chemically resolved $PM_{2.5}$ data have been collected across Canada through the National Air Pollution Surveillance network in the past decade. 24-hr time integrated $PM_{2.5}$ collected at seven urban and two rural sites during 2010-2016 were analyzed to characterize geographical and seasonal patterns and associated potential causes. Site-specific seven-year mean gravimetric $PM_{2.5}$ mass concentrations ranged from 5.7 to 9.6 μg/m^3. Seven-year mean concentrations of SO_4^{2-}, NO_3^-, NH_4^+, organic carbon (OC), and elemental carbon (EC) were in the range of 0.68 to 1.6, 0.21 to 1.5, 0.27 to 0.71, 1.1 to 1.9, and 0.37 to 0.71 μg /m^3, accounting for 10.8%-18.1%, 3.7%-16.7%, 4.7%-7.4%, 18.4%-21.0%, and 6.4%-10.6%, respectively, of gravimetric $PM_{2.5}$ mass. $PM_{2.5}$ and its five major chemical components showed higher concentrations in southeastern Canada and lower values in Atlantic Canada, with the seven-year mean ratios between the two regions being on the order of 1.7 for $PM_{2.5}$ and 1.8-7.1 for its chemical components. When comparing the concentrations between urban and rural sites within the same region, those of SO_4^{2-} and NH_4^+ were comparable, while those of NO_3^-, OC, and EC were around 20%, 40%-50%, and 70%-80%, respectively, higher at urban than rural sites, indicating the regional scale impacts of SO_4^{2-} and NH_4^+ and effects of local sources on OC and EC. Monthly variations generally showed summertime peaks for SO_4^{2-} and wintertime peaks for NO_3^-, but those of NH_4^+, OC, and EC exhibited different seasonality at different locations.

1. Introduction

Fine particulate matter ($PM_{2.5}$) has harmful impacts on public health, air quality, and visibility, and plays a role in

* Corresponding author.
E-mail: leiming.zhang@canada.ca (L. Zhang).
** Work conducted while being a visiting fellow at Environment and Climate Change Canada.

https://doi.org/10.1016/j.jes.2020.09.035
1001-0742/

climate change by affecting the Earth's radiation budget (Bahadur et al., 2012; Wang et al., 2017; Zhang et al., 2016). Secondary water-soluble inorganic ions including sulfate (SO_4^{2-}), nitrate (NO_3^-), and ammonium (NH_4^+) (hereafter referred to as SNA), and carbonaceous components, mainly organic carbon (OC) and elemental carbon (EC), are major constituents of $PM_{2.5}$ in global megacities (Cheng et al., 2016). SNA are mostly formed from their respective gaseous precursors, namely SO_2, NO_x and NH_3, through gaseous and aqueous phase reactions (Reid and Aherne, 2016; Squizzato et al., 2018). Due to their hygroscopicity and solar radiation scattering properties, SNA play important roles in visibility impairment or haze occurrence and heavy air pollution events (Qiao et al., 2019; Tian et al., 2017; Wang et al., 2018; Zheng et al., 2015). EC or black carbon, which is directly emitted from biomass burning and vehicles, strongly absorbs solar radiation, and is a major contributor to climate forcing, second only to CO_2 (Bahadur et al., 2011). OC can also be released directly from primary sources or formed through oxidation of volatile organic compounds (VOCs). A fraction of OC, termed brown carbon, absorbs solar radiation and consequently influences radiative forcing (Wang et al., 2020; Wang et al., 2014). OC contains many toxic species that can cause adverse effects on human health (Hvidtfeldt et al., 2019).

Quantifying the above-mentioned impacts of $PM_{2.5}$ requires long-term measurements of chemically-resolved $PM_{2.5}$ data at multiple locations. In Canada, such data have been collected over the last decade at major urban and rural areas within the National Air Pollution Surveillance (NAPS) network (Dabek-Zlotorzynska et al., 2011). There are also several other similar networks worldwide collecting $PM_{2.5}$ speciation data, such as IMPROVE and the Chemical Speciation Network across United States (Solomon et al., 2014), the Southeastern Aerosol Research and Characterization network (SEARCH) in southeastern US (Hansen et al., 2003), the Campaign on Atmospheric Aerosol Research network (CARE) in China (Xin et al., 2015), and the European Aerosol Cloud Climate and Air Quality Interactions project (EUCAARI) (Hamburger et al., 2011).

Data collected in the above-mentioned three networks in the US have been analyzed extensively to reveal seasonal and spatial trends (Chan et al., 2018; Hand et al., 2013; Hand et al., 2012), identify sources and quantify associated contributions (Hand et al., 2013; Hand et al., 2014; Masiol et al., 2019; Schichtel et al., 2008; Thurston et al., 2011; Zhai et al., 2017), explore chemical formation processes (Shah et al., 2018), and investigate long-term trends (Blanchard et al., 2016; Malm et al., 2017; McClure and Jaffe, 2018; Ridley et al., 2018), of $PM_{2.5}$ and its major chemical components. Studies focusing on NAPS $PM_{2.5}$ chemical speciation data were rather limited (Bari and Kindzierski, 2016; Dabek-Zlotorzynska et al., 2011; Jeong et al., 2019; Sofowote et al., 2015a, 2012b). Among these studies, only one study focused on the national scale, for the period 2003-2008 (Dabek-Zlotorzynska et al., 2011), an earlier period than examined here. Considering that anthropogenic emissions of gaseous precursors (mostly SO_2 and NOx) have been reduced significantly across Canada since 2006 (Canada's Air Pollutant Emissions Inventory Report 2019), it is necessary to update our knowledge on the spatiotemporal patterns of $PM_{2.5}$ at the national scale using more recently collected data.

In the present study, nine monitoring sites in the NAPS network that have seven year (2010-2016) complete $PM_{2.5}$ speciation data were chosen for analyzing spatial and seasonal variations of $PM_{2.5}$ and its major chemical components. Specific goals of the present study include (1) revealing the geographical patterns of $PM_{2.5}$ and its major chemical components by grouping the nine sites into three regions (Atlantic, Southeastern and Western Canada), (2) characterizing their seasonal patterns by analyzing seven-year mean monthly data, (3) identifying the major causes of the typical seasonal patterns at individual sites, and (4) exploring the relative importance between regional transport and local sources of pollutants in Southeastern Canada by comparing two pairs of neighboring urban-rural sites.

2. Methodology

2.1. Monitoring sites

In the present study, nine monitoring sites from the NAPS network having $PM_{2.5}$ speciation data of the five major chemical components (SO_4^{2-}, NO_3^-, NH_4^+, OC, and EC) during 2010-2016 were selected for analysis (**Fig. 1 and Table S1**). These include two urban sites (Halifax, NS; Saint John, NB) in Atlantic Canada, three urban (Montreal, QC; Ottawa, ON; Toronto, ON) and two rural sites (Saint Anicet, QC; Simcoe, ON) in southeastern Canada, and two urban sites (Edmonton, AB; Burnaby South, BC) in western Canada. Simcoe is located about 120 km southwest of metropolitan Toronto, while Saint Anicet is situated 70 km southwest of downtown Montreal. Toronto-Simcoe and Montreal-Saint Anicet were considered to be urban-rural pairs to capture the impact of urban sources on the regional air quality.

2.2. Sampling and analytical methods

The sampling protocol used in this study and analytical methods for $PM_{2.5}$ mass and its major chemical components were previously described in Dabek-Zlotorzynska et al. (2011). Briefly, 24hr integrated $PM_{2.5}$ samples starting at midnight were collected using a speciation sampler (Partisol Model 2300, Thermo Scientific Inc.) on every third or sixth day. Three parallel cartridges (A, B, C) were used to collect $PM_{2.5}$ samples at a flow rate of 10 L/min. A field blank was loaded into cartridge D for the same length of time as active samples. Cartridge A was loaded with a pre-fired quartz filter for OC and EC analysis. A Teflon filter and a pre-fired quartz backing filter were loaded into Cartridge B in series, where the Teflon filter was used for $PM_{2.5}$ mass analysis while the backup quartz filter was analyzed for positive carbonaceous sampling artifacts arising from adsorption of gas phase carbon species. Cartridge C was composed of two denuders and two filters. One denuder was coated with citric acid to collect gaseous NH_3, and the other one was coated with Na_2CO_3 for trapping gaseous HNO_3 and SO_2. The front Teflon filter in Cartridge C was used for water-soluble inorganic ions, followed by a Nylon backup filter to collect nitrate loss during sampling.

All $PM_{2.5}$ samples were analyzed in the laboratory of the Air Quality Research Division of Environment and Climate

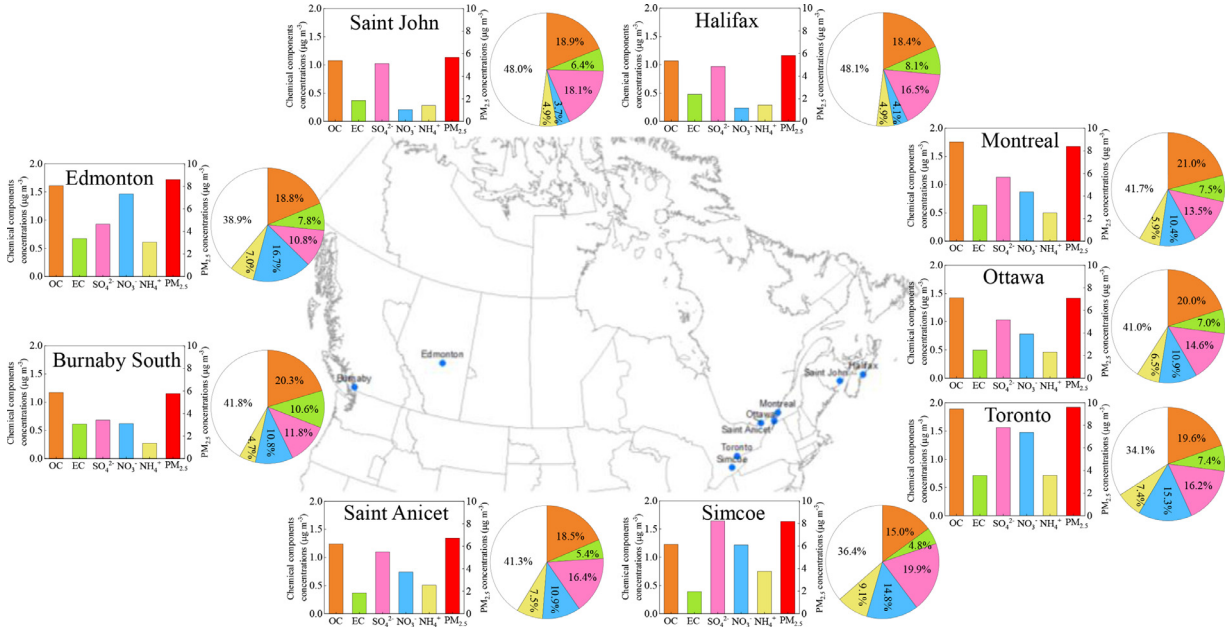

Fig. 1 – Seven-year (2010-2016) mean concentrations of $PM_{2.5}$ (μg/m^3) and major chemical components as well as their percentage (%) contributions to $PM_{2.5}$ at nine monitoring sites. The colors in the pie charts are the same as in the bar graphs except with additional white areas representing other chemical components in $PM_{2.5}$.

Change Canada in Ottawa. $PM_{2.5}$ mass was determined gravimetrically by weighing the Teflon filters in Cartridge B before and after the sampling under controlled conditions (e.g., relative humidity of 40% ± 5% and temperature of 23±3°C). Major water-soluble inorganic ions (SO_4^{2-}, NO_3^-, and NH_4^+) were analyzed from the Teflon filter in Cartridge C using ion chromatography (IC), and NO_3^- loaded on the backup Nylon filter was also determined to correct for volatile NO_3^-. In addition, the extracts from the two denuders were also analyzed by IC to quantify NH_3 and $PM_{2.5}$ acidic gaseous precursors (SO_2 and HNO_3). OC and EC loaded on the quartz filters in Cartridge A and B were analyzed using a DRI Model 2001 Thermal/Optical Carbon Analyzer (Atmoslytic Inc. Calabasas, CA) according to the thermal optical reflectance (TOR) method (Chow et al., 2007). The particulate OC was corrected by subtracting the OC content of the backup quartz filter in cartridge B from that in Cartridge A. Levoglucosan loaded on the Teflon filter was first extracted in water and then measured using an IC equipped with pulsed amperometric detection. Major elements and trace metals were also analyzed, but these data are not reported in this manuscript. Additional details regarding analytical methods for $PM_{2.5}$ mass and its major chemical components can be found elsewhere (Dabek-Zlotorzynska et al., 2019; Dabek-Zlotorzynska et al., 2011; Jeong et al., 2020; Jeong et al., 2013). Furthermore, metadata and method detection limits (MDL) can be downloaded from the NAPS website (http://data.ec.gc.ca/data/air/monitor/national-air-pollution-surveillance-naps-program/).

Values below MDL were replaced by half of the MDL for each chemical component in $PM_{2.5}$. All missing data and those days with evident wildfire events characterized by extremely high levoglucosan concentrations were excluded from the statistical analysis. In any given month, monthly mean concentration of individual chemical species at a monitoring site was first calculated when a minimum 50% completeness of the daily data was satisfied. Annual mean concentration was then calculated if there were eight valid monthly mean values spreading over all the seasons. Finally, the seven-year mean concentration was obtained from the seven annual mean values. The reconstructed $PM_{2.5}$ mass concentrations that were typically calculated from major chemical components (Dabek-Zlotorzynska et al., 2011), such as $(NH_4)_2SO_4$, NH_4NO_3, organic matter (OM), EC, crustal material, trace oxidized metals, and particle bound water, were not conducted in the present study. The percentage fractions discussed below were estimated based on the ratios of the measured SO_4^{2-}, NO_3^-, NH_4^+, OC, and EC to the measured gravimetric $PM_{2.5}$ mass, while crustal material, trace oxidized metals, particle bound water, as well as the other elements in OM (the factor for OM/OC ratio) were considered together as "others" to constitute the remaining fractions in $PM_{2.5}$.

2.3. *Gaseous pollutants concentrations and emission inventory*

Secondary aerosols are produced from their gaseous precursors through photochemical and/or heterogeneous reactions. Therefore, hourly gaseous pollutants such as NO_2 were also retrieved from NAPS network. Hourly data were then averaged to daily concentrations to correspond with the sampling intervals of the $PM_{2.5}$ chemical species. Emissions were obtained from Canada's Air Pollutants Emissions Inventory (APEI) (https://pollution-waste.canada.ca/air-emission-inventory). Major air pollutant emissions including SO_2, NOx, NH_3, and VOCs were available during 2010-2016 on a yearly basis at the provincial level.

Table 1 – Seven-year (2010-2016) mean concentrations (±standard deviation) for $PM_{2.5}$ and its five major chemical components at nine monitoring sites

Region	Sampling site	Site type	Mean concentrations (± standard deviation) (μg/m³)					
			$PM_{2.5}$	SO_4^{2-}	NO_3^-	NH_4^+	OC	EC
Atlantic Canada	Halifax, NS	urban	5.8±0.58	0.97±0.25	0.24±0.04	0.29±0.08	1.1±0.09	0.48±0.14
	Saint John, NB	urban	5.7±0.41	1.0±0.11	0.21±0.02	0.28±0.04	1.1±0.19	0.37±0.13
Southeastern Canada	Montreal, QC	urban	8.4±0.69	1.1±0.19	0.87±0.12	0.50±0.08	1.8±0.15	0.64±0.15
	Ottawa, ON	urban	7.1±0.91	1.0±0.19	0.78±0.17	0.46±0.08	1.4±0.21	0.49±0.12
	Toronto, ON	urban	9.6±0.98	1.6±0.28	1.5±0.26	0.71±0.14	1.9±0.30	0.71±0.12
	Saint Anicet, QC	rural	6.7±0.99	1.1±0.24	0.74±0.21	0.51±0.12	1.2±0.16	0.37±0.13
	Simcoe, ON	rural	8.2±0.74	1.6±0.36	1.2±0.26	0.75±0.17	1.2±0.13	0.39±0.09
Western Canada	Edmonton, AB	urban	8.6±1.1	0.93±0.14	1.5±0.50	0.61±0.18	1.6±0.21	0.67±0.17
	Burnaby South, BC	urban	5.8±0.48	0.68±0.14	0.62±0.11	0.27±0.07	1.2±0.13	0.61±0.12

3. Results and discussion

3.1. $PM_{2.5}$

3.1.1. *Geographical patterns*

During the 2010-2016 period, annual mean concentrations of $PM_{2.5}$ were in the range of 5.0-6.6 μg/m³ in Halifax, 5.0-6.2 μg/m³ in Saint John, 7.3-9.2 μg/m³ in Montreal, 5.3 -8.0 μg/m³ in Ottawa, 8.1-10.6 μg/m³ in Toronto, 7.4-10.9 μg/m³ in Edmonton, and 4.9-6.4 μg/m³ in Burnaby South (near Vancouver, BC). These values were mostly below the 2015 Canadian Ambient Air Quality Standards (CAAQS) of 10 μg/m³ except during four years (2010, 2011, 2012, 2015) in Toronto and one year (2010) in Edmonton with slightly higher values (10-11 μg/m³). Note that the annual mean concentrations of $PM_{2.5}$ in this study were calculated based on filter sampling with the frequency of 1 in 3 days or 1 in 6 days rather than daily, which were likely to have some biases from daily monitoring of $PM_{2.5}$ using continuous instruments. $PM_{2.5}$ levels in Toronto were comparable with those in US megacities such as New York, Atlanta, and Chicago, but were around 10 times lower than those in some polluted megacities in the Indo-Gangetic Plain and China, such as Delhi and Xi'an (Cheng et al., 2016).

Site-specific seven-year (2010-2016) mean concentration (±standard deviation) of $PM_{2.5}$ varied from 5.7±0.41 to 9.6±0.98 μg/m³ (**Table 1 and Fig. 1**), corresponding to Saint John and Toronto, respectively. $PM_{2.5}$ concentrations were generally higher in southeastern Canada (including the two rural sites) than Atlantic Canada. In western Canada, $PM_{2.5}$ concentration was 50% higher in Edmonton than Burnaby South. Regional and local emissions as well as coastal versus inland locations played a role in causing site differences in $PM_{2.5}$ concentrations. For example, provincial-level emissions of gaseous precursors were the highest in Alberta, followed by Ontario and Quebec, and the lowest in Atlantic Canada (**Fig. S1**). The size of the city is much larger for Toronto than the other cities, which tends to have emission sources from vehicular traffic and construction. Halifax, Saint John, and Burnaby South are coastal cities, and an increased influence from clean marine air masses could lead to low $PM_{2.5}$ concentrations. The phenomenon of lower $PM_{2.5}$ concentrations at coastal than inland sites was also observed elsewhere, e.g., 30%-40% lower at Gulfport than North Birmingham during 2009-2012 in the southeastern US (Hidy et al., 2014). As for the paired urban-rural sites in Ontario and Quebec, $PM_{2.5}$ concentrations were only about 20% higher at urban than the corresponding rural sites (Toronto versus Simcoe and Montreal versus Saint Anicet), implying regional emissions dominated pollution of $PM_{2.5}$.

3.1.2. *Seasonality*

Seven-year average monthly variations of $PM_{2.5}$ are displayed in Fig. 2. Generally, the highest monthly $PM_{2.5}$ concentrations were observed in summer across Canada except in Edmonton and Montreal, while the lowest appeared in April and/or October. Due to the stronger solar intensities and higher temperatures, more secondary aerosol formation was probably responsible for the increased $PM_{2.5}$ concentrations in summer, in particular in Atlantic Canada. This is supported by the maximum concentrations of SO_4^{2-}, NH_4^+, and OC occurring in July. In southeastern Canada, higher $PM_{2.5}$ concentrations were observed in both summer and winter and lower values in spring and fall. The highest monthly $PM_{2.5}$ concentrations were in January in Montreal and Ottawa due to the influence of wood burning for residential heating, as evidenced by the very high EC and levoglucosan concentrations. The peak in July in Toronto may be partly associated with transboundary air masses from neighboring US. In Edmonton, higher $PM_{2.5}$ concentrations were observed during cold seasons, generally from November to March, which were about 50% higher than those in the other months. This seasonal pattern was related to the frequent occurrence of temperature inversions and calm wind conditions in winter along with the dry climate limited dispersion and deposition of the primary pollutants, which in turn enhanced secondary aerosol formation due to the increased time residence of gaseous precursors in the air (Myrick et al., 1994). In addition, combustion emissions for heating in winter were likely responsible for the high $PM_{2.5}$ concentrations, which could be found from the highest EC and levoglucosan concentrations. Monthly variations of $PM_{2.5}$ in Burnaby South were small with a weak peak in August. Wind speeds at this site changed little with season and monthly variations in temperature were smallest among all the sites (**Fig. S2**). The two rural sites displayed consistent monthly variations of $PM_{2.5}$

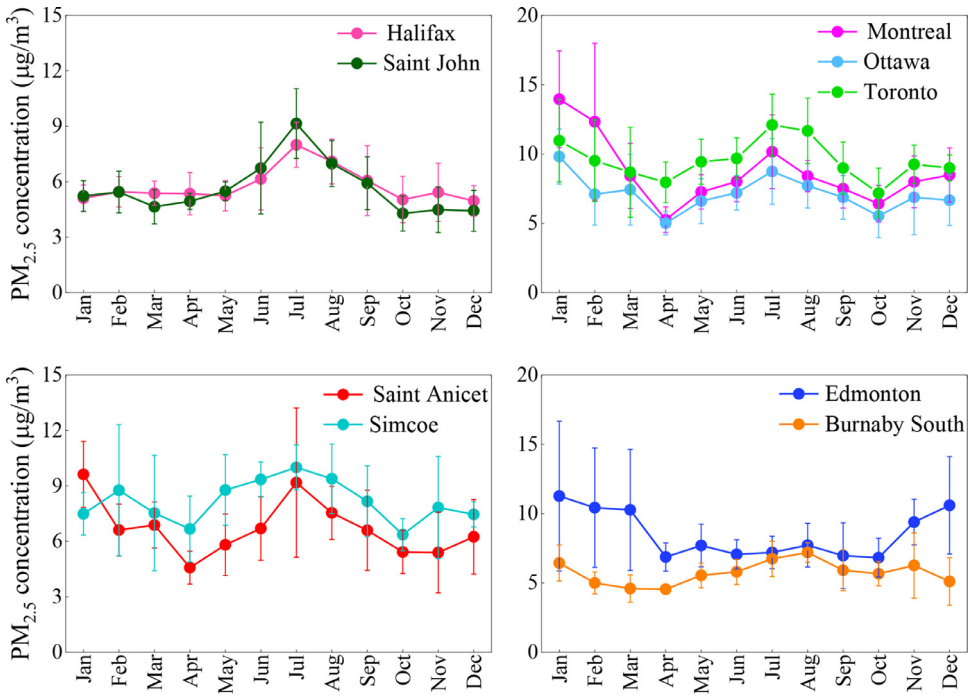

Fig. 2 – Seven-year (2010-2016) mean monthly variations of $PM_{2.5}$ concentrations and standard deviation at nine monitoring sites.

with their respective paired urban sites, with the maximum value in January in Saint Anicet and in July in Simcoe.

3.2. *Inorganic ions*

3.2.1. *Geographical patterns*

Site-specific seven-year mean concentrations ranged from 0.68 to 1.6 μg/m^3 for SO_4^{2-}, from 0.21 to 1.5 μg/m^3 for NO_3^-, and from 0.27 to 0.71 μg/m^3 for NH_4^+ at the seven urban sites (Table 1). Averaging the seven urban sites together would have 1.0±0.27, 0.81±0.52, and 0.45±0.17 μg/m^3 for SO_4^{2-}, NO_3^-, and NH_4^+, respectively.

Mean SO_4^{2-} concentrations were generally higher in southeastern and Atlantic Canada than western Canada. The highest concentration of SO_4^{2-} occurred in Toronto while the lowest in Burnaby South, with a factor of 2.3 difference. Note that while the other four major constituents in $PM_{2.5}$ were substantially lower in the Atlantic region (Halifax and Saint John) than the other urban sites, SO_4^{2-} concentrations were comparable. This is due to the relatively high concentrations of SO_2 precursor at the two urban sites in Atlantic Canada (Fig. 3), which were likely caused by power plants in close proximity to the monitoring sites. With the exception of Ottawa and Burnaby South, the SO_2 concentration in Toronto was comparable or even lower than the remaining four cities, nevertheless, the SO_4^{2-} concentration in Toronto was the highest among the seven monitoring sites. This phenomenon was likely due to the long-range transport of SO_4^{2-} from combustion and industrial sources in neighboring US (Blanchard et al., 2013; Jeong et al., 2013). Other factors such as available oxidants and cloud processing also influence SO_4^{2-} formation, but the impact of these processes on the spatial distributions of SO_4^{2-} cannot be explored using the current data set. A detailed air quality modeling simulation may shed more lights on this issue.

In contrast to the small spatial variabilities in SO_4^{2-} concentrations mentioned above, the mean NO_3^- concentrations varied by nearly an order of magnitude across Canada, demonstrating the dominant role of local emissions of NOx on NO_3^- levels. More than 70% of NO_x emissions were from the transportation sector in most Canadian provinces (except Alberta, **Fig. S1**). Cities with heavy traffic typically showed relatively high NO_3^- concentrations, e.g., the highest concentration of NO_3^- and NO_2 were both observed in Toronto (Fig. 3). However, the two coastal sites, Halifax and Burnaby South, did not show consistent spatial trends between NO_2 and NO_3^- concentrations. e.g., the concentrations of NO_2 in Halifax were comparable to Montreal, whereas NO_3^- concentrations in Halifax was almost 3.7 times lower than in Montreal. This discrepancy between the regions could be due to a few reasons, such as different meteorological conditions or different available ammonia amounts. Ammonium availability index (*J*), which is defined as the molar ratio of NH_4^+ to the sum of SO_4^{2-} and NO_3^- ($J = [NH_4^+]/(2[SO_4^{2-}]+[NO_3^-])$), could be used to identify the degree of neutralization (Chu, 2004). $J \geq 1$ indicates that SO_4^{2-} and NO_3^- could be fully neutralized by NH_4^+, while $J < 1$ means NH_4^+-poor situation where NH_3 prefers to react with H_2SO_4 and the excess NH_3 will neutralize HNO_3. The seven-year mean J value was slightly smaller in Halifax (0.66) than Montreal (0.74), implying potential less NO_3^- formation in Halifax. Annual precipitation amounts were also much higher in Halifax than in inland cities (**Fig. S3**), knowing that precip-

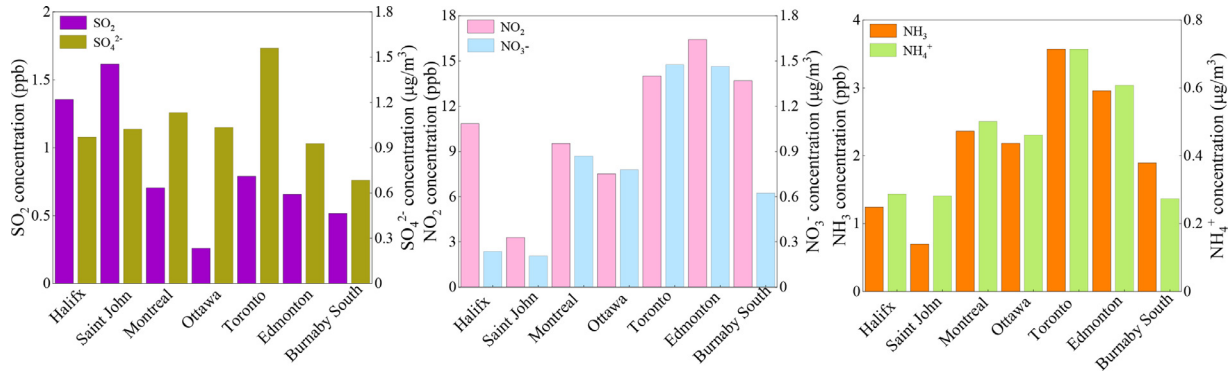

Fig. 3 – Seven-year (2010-2016) mean concentrations of SO_2 *vs.* SO_4^{2-}, NO_2 *vs.* NO_3^-, and NH_3 *vs.* NH_4^+ at seven urban sites.

itation scavenging is faster for HNO_3 and NO_3^- than NO_2 because of their different solubility. The concentrations of NO_3^- were relatively lower in Burnaby South likely because of the higher annual mean temperatures compared to other cities, noting that high temperature enhances NH_4NO_3 evaporation.

The geographical patterns of NH_4^+ concentrations followed those of SO_4^{2-} concentrations, but were slightly different from those of NO_3^- concentrations. The highest mean NH_4^+ concentration was observed in Toronto and the lowest in Burnaby South. The seven-year mean J value ranged from 0.63 in Saint John to 0.79 in Edmonton, indicating that the aerosol was under the NH_4^+-poor condition at all sites in Canada, which explains the phenomenon that the geographical patterns of NH_4^+ followed more of those of SO_4^{2-} than NO_3^-. Site-mean NH_4^+ and NH_3 concentrations correlated strongly with each other, e.g., with an R^2 value of 0.86 if considering all the sites together and an even higher R^2 value of 0.97 if excluding the Burnaby South site (**Fig. S4**). Such a strong correlation indicated that NH_3 level, which is mostly controlled by the intensity of source emission, was the dominant factor controlling NH_4^+ concentrations in Canada. The deviation of the Burnaby South from the linear curve implied that additional factors such as thermodynamic equilibrium of NH_4NO_3, besides NH_3 concentration, should also have affected NH_4^+ concentrations. The relatively high temperatures in Burnaby South should have shifted NH_4NO_3 to the gaseous NH_3 and HNO_3 and thus reduced the concentrations of particulate NH_4^+ and NO_3^-.

As shown in **Figs. S5** and **S6**, comparable concentrations of both SO_2 and SO_4^{2-} were seen for paired urban-rural sites. Furthermore, both Saint Anicet and Simcoe were classified as regional background sites in NAPS, and thus the small spatial variations in SO_4^{2-} between urban and rural sites highlighted the regional scale impact of SO_4^{2-}. In contrast, NO_2 concentrations were almost 3 times lower at rural sites than their paired urban sites due to significant vehicle emissions in cities, while NO_3^- concentrations were only about 20% lower due to the longer life time of NO_3^- than NO_2 and the regional-scale transport of NO_3^-. NH_3 is typically from agricultural sources such as fertilizer application and livestock. The comparable or even higher NH_3 concentrations in Montreal and Toronto than the corresponding rural sites implied the existence of additional NH_3 sources inside cities, such as transportation, incineration and waste management. Similar to the cases of SO_4^{2-} and NO_3^-, comparable concentrations of NH_4^+ were observed at the paired urban-rural sites, again emphasizing the homogeneity in secondary inorganic aerosol concentrations in southeastern Canada.

3.2.2. *Seasonality*

Variations of monthly mean SO_4^{2-} concentrations, defined as the ratio of maximum to minimum monthly mean at a given site, were on the order of a factor of 1.6-3.0 across the sites, with the largest monthly variability in Burnaby South and the smallest variability in Halifax. Those of NO_3^- were on the order of a factor of 2.0-14.5 with the largest value in Ottawa and Edmonton and smallest one in Halifax, and those for NH_4^+ were a factor of 1.9-7.4 with the largest value in Edmonton and the smallest one in Burnaby South.

SO_4^{2-} concentrations were generally higher in summer than in the other seasons, except in Edmonton where higher values appeared in winter (**Fig. 4**). The summer SO_4^{2-} maximum was also observed in the US and Europe (Hand et al., 2012; Salameh et al., 2015). High temperature and strong solar radiation in summer enhance the secondary SO_4^{2-} formation at all sites. Similar to the seasonality of $PM_{2.5}$, the highest concentration of SO_4^{2-} in summer in Toronto was also related to the long-range transport from neighboring US, and the maximum of SO_4^{2-} in winter in Edmonton was possibly due to unfavorable diffusion conditions.

NO_3^- also exhibited pronounced monthly variations, but with opposite trends to those of SO_4^{2-}, e.g., with the highest monthly concentrations in winter and the lowest values in summer at all sites. The seasonal patterns of NO_3^- might be caused by several factors. The low temperatures in winter shifted the thermodynamic equilibrium of NH_4NO_3 from the gas phase to particulate phase, resulting in increased particulate NO_3^- formation. Moreover, heterogeneous processes may also contribute to NO_3^- formation in winter since relative humidity above 75% often occurred during cold days (**Fig. S2**). These seasonal trends of NO_3^- with maximum concentration in winter but minimum level in summer were also commonly observed worldwide (Hand et al., 2012; Masiol et al., 2015; Ricciardelli et al., 2017; Wang et al., 2018).

NH_4^+ concentrations showed less pronounced seasonal trends than those of SO_4^{2-} and NO_3^-. The seasonal pattern of NH_4^+ was also related to the ammonium availability index. In Atlantic Canada, the monthly variations of NH_4^+ fol-

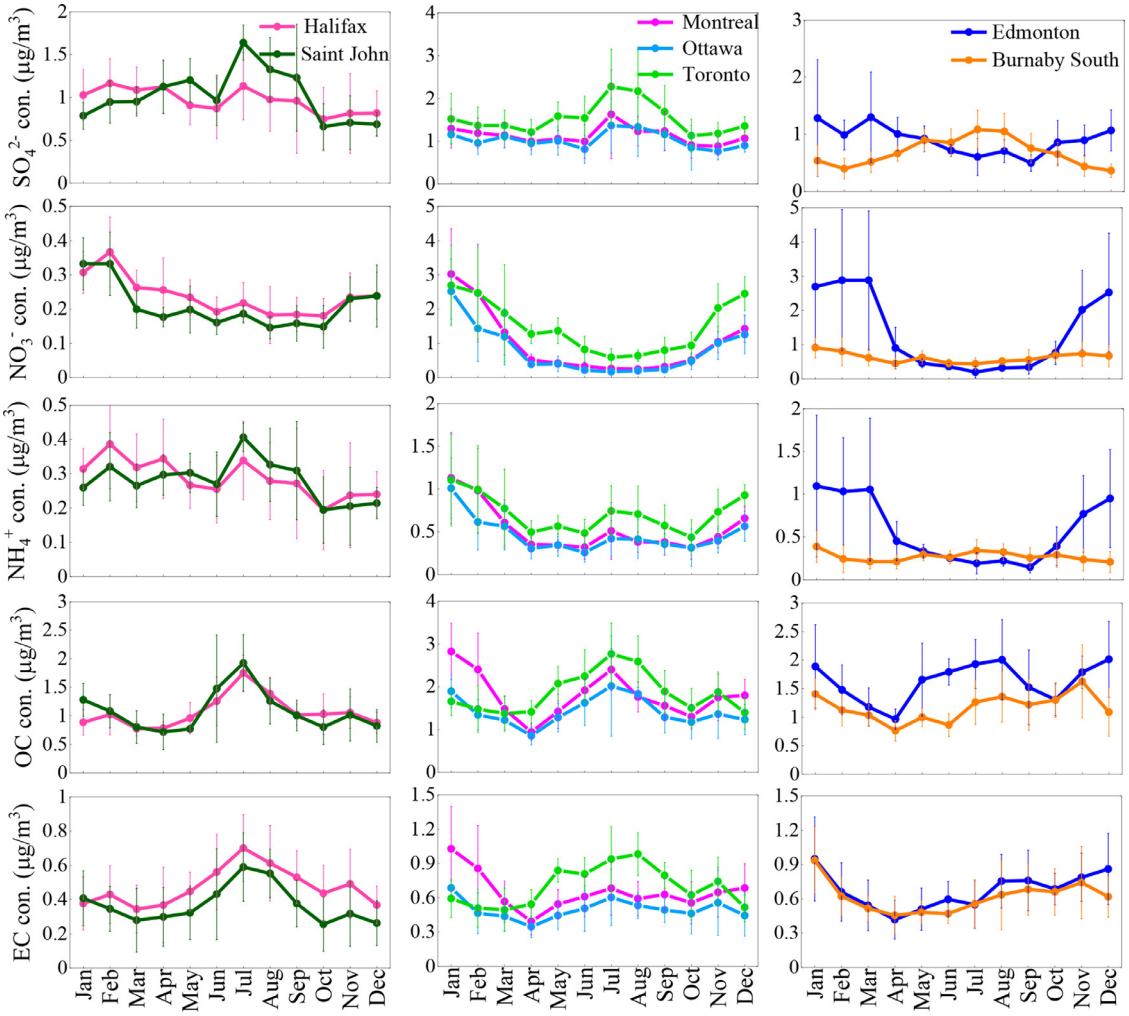

Fig. 4 – Seven-year (2010-2016) mean monthly variations of SO_4^{2-}, NO_3^-, NH_4^+, OC, and EC concentrations and standard deviation at nine monitoring sites.

lowed those of SO_4^{2-} with maximum concentration in summer in Saint John and in both summer and winter in Halifax, which was due to the relatively high NH_3 deficiency in this region. As shown in **Fig. S7**, the molar ratio of NH_4^+ to SO_4^{2-} was between 1.0 and 2.0 all year round in Atlantic Canada, meaning that NH_3 could not fully neutralize SO_4^{2-} and thus its concentration was dominantly affected by the SO_4^{2-}. Nevertheless, the seasonal pattern of NH_4^+ was consistent with those of NO_3^- in Edmonton with a peak in winter, where the molar ratio of NH_4^+ to SO_4^{2-} was much higher than 2.0 all year round except in summer and thus SO_4^{2-} played a minor role on the seasonality of NH_4^+. In southeastern Canada, the monthly variations of NH_4^+ were controlled by both SO_4^{2-} and NO_3^-, presenting high concentrations in both summer and winter.

3.2.3. *SNA fractions in $PM_{2.5}$*

SNA in total contributed on average 25.5%-38.8% of $PM_{2.5}$ at the seven urban sites, with the highest average percentage in Edmonton and the lowest in Atlantic Canada. Nearly half of SNA, or 10.8%-18.1% of $PM_{2.5}$, was from SO_4^{2-} (Fig. 1), with the highest percentage observed in Saint John. The fractions of SO_4^{2-} in $PM_{2.5}$ were generally lower in western Canada than in the other regions. While the lower fraction of SO_4^{2-} in Burnaby South was ascribed to the high fractions of carbonaceous components, which accounted for more than 30% of $PM_{2.5}$. The lower fraction of SO_4^{2-} in Edmonton was actually due to its significantly high concentrations of OC and NO_3^- since SO_4^{2-} concentrations in Edmonton were comparable to those at most of the other urban sites. Seasonal variations of SO_4^{2-} fractions were low, e.g., less than a factor of 1.3 (**Fig. S8**). The fractions of NO_3^- in $PM_{2.5}$ ranged from 3.7% in Atlantic Canada to 16.7% in Edmonton for the seven-year average. The fractions of NO_3^- in $PM_{2.5}$ were in the range of 2.2%-7.1% in summer and 5.4%-26.3% in winter, or seasonal variation of a factor of 1.9-8.3, depending on site. The large seasonal differences in NO_3^- fractions were due to the strong seasonal variations in NO_3^- concentrations. NH_4^+ only accounted for 4.7%-7.4% of $PM_{2.5}$ concentrations. Similar to NO_3^-, the contribution of NH_4^+ to $PM_{2.5}$ was higher in winter (4.8%-9.1%) than summer (3.0%-5.7%) at all sites. The substantially higher contributions of both NO_3^- and NH_4^+ to $PM_{2.5}$ in winter were primarily ascribed to low temperatures that facilitated the formation of NH_4NO_3.

3.3. OC and EC

3.3.1. Geographical patterns

Site-specific mean concentrations ranged from 1.1±0.09 to 1.9±0.30 μg/m^3 for OC and from 0.37±0.13 to 0.71±0.12 μg/m^3 for EC at the seven urban sites, and the seven-site average OC and EC values were 1.4±0.33 and 0.57±0.12 μg/m^3, respectively (Table 1). Among the five major chemical components of $PM_{2.5}$ discussed in the present study, OC and EC showed relatively smaller spatial variabilities (a factor of 1.8 -1.9). Similar to the geographical patterns of $PM_{2.5}$, higher concentrations of OC and EC were observed in southeastern Canada and Edmonton than Atlantic Canada. Both OC and EC showed the highest concentrations in Toronto and the lowest in Saint John. Contrary to the extremely low concentrations of the other major chemical components observed in Halifax and Burnaby South, relatively high concentrations of EC were seen at these sites, which were probably related to shipping emissions due to their proximity to the Halifax Harbor and port of Vancouver, respectively (Wiacek et al., 2018).

OC/EC ratio can be used to indicate sources, with lower values reflecting primary emissions being dominant contributors to both OC and EC, and higher values indicating additional contributions from the secondary formation of OC (Chow et al., 1996). Mean OC/EC ratios varied from 1.9 to 2.9 at the seven urban sites. The lowest ratio of 1.9 in Burnaby South indicates the dominant role of primary emissions to OC and EC concentrations because this site was mainly influenced by vehicle and shipping emissions, which was supported by the relatively high NO_2 and EC concentrations. The high ratios of around 2.8 at the three urban sites in southeastern Canada and Saint John imply the important contribution of secondary aerosol formation to OC concentration.

For the paired urban-rural sites, OC and EC concentrations were 1.4 and 1.7 times higher, respectively, at urban than rural sites. The larger urban-rural differences in OC and EC concentrations than the secondary inorganic ions discussed above indicated the important role of local primary emissions on OC and EC concentrations. Thus, while the impact of secondary inorganic ions in southeastern Canada was at the regional scale, those of OC and EC were more local in nature.

3.3.2. Seasonality

Monthly mean variations of OC and EC concentrations were both on the order of a factor of 2.0-3.0 across the sites. The maximum concentrations of OC occurred in summer at five urban sites and in winter at two urban sites (Montreal and Burnaby South), while the minimum occurred in April and/or October at all the sites (Fig. 4). The high OC concentrations in summer can be explained by two factors. Firstly, high isoprene and α-pinene emissions combined with high O_3 concentrations, both of which were promoted by high temperatures and strong solar radiation, produced more secondary organic aerosols (SOA) in summer than in other seasons. Secondly, wildfires in summer likely produced more OC as indicated by the relatively high concentrations of levoglucosan, a chemical marker indicative of biomass burning (Bhattarai et al., 2019), in June or July. For example, wildfire smoke has been proposed as the cause of the high summertime OC concentrations in Edmonton (Bari and Kindzierski, 2016). The higher concentrations of OC in summer have also been observed at urban and rural sites in eastern US and rural sites in western US (Hand et al., 2013; Hand et al., 2012), which were attributed to wildfires as well as enhanced SOA formation. The highest seasonal OC concentrations in winter in Montreal were probably caused by wood burning for residential heating, as supported by the extremely high levoglucosan concentrations, e.g., nearly one order of magnitude higher in January than between May and August (**Fig. S9**). In Burnaby South, the relative humidity was typically higher than 90% in winter, which is conducive to SOA production possibly through aqueous-phase processes (Ge et al., 2012).

Monthly variations of EC concentrations were similar to those of OC. The maximum concentrations were observed in January in western Canada. Interestingly, the maximum concentrations of EC were observed in summer, like OC, at all sites in Atlantic Canada and southeastern Canada except Montreal, but EC is commonly from primary emissions rather than secondary aerosol formation. Looking at the emission inventory of black carbon, it can be clearly seen that biomass burning and transportation fuel emissions, in particular diesel vehicle emissions, were the two major contributors to black carbon. The increased shipping emissions in Atlantic Canada during warm periods may have influenced EC concentrations at the near port monitoring sites, which could partly explain the higher EC concentrations in summer in Halifax and Saint John (Gibson et al., 2013; Wiacek et al., 2018). As for the sites in southeastern Canada, high EC concentrations in summer could be mainly caused by long-range transport of pollutants, similar to the findings by Healy et al. (2017) who showed that the maximum seasonal concentration of black carbon in summer in Ontario was mainly associated with transboundary pollution originating from Michigan, Ohio, Pennsylvania and New York in the US.

3.3.3. OC and EC fractions in $PM_{2.5}$

The sum of OC and EC accounted for 25.4%-30.9% of $PM_{2.5}$ on average at the seven urban sites, of which OC contributed 18.4%-21.0% and EC 6.4%-10.6%. Seasonally, OC fractions in $PM_{2.5}$ were typically higher in summer than in winter at all the sites except Burnaby South where the higher fractions appeared in winter (**Fig. S8**). EC fractions in $PM_{2.5}$ were highest in Halifax and Burnaby South due to the influence of shipping emissions and were lowest in Saint John because of few local emission sources. In Burnaby South, similar to the case of OC, EC fractions in $PM_{2.5}$ were higher in winter (13.6%) and lower in summer (7.7%). At the other sites, seasonal variations of EC fractions in $PM_{2.5}$ were relatively flat, ranging from 5.0%-8.7% in summer and 4.1%-8.2% in winter.

4. Conclusions

Spatial variations of $PM_{2.5}$ were on the order of a factor of 1.7 between the seven urban sites based on seven-year average data, and those of its major chemical components (SO_4^{2-}, NO_3^-, NH_4^+, OC, and EC) were on the order of a factor of 1.8-7.1. The highest concentrations of $PM_{2.5}$ and its major chemical components were observed in Toronto, and were associated with high local emissions produced by its large popula-

tion and developed economy as well as long-range transport of pollutants from neighboring states in the US. In contrast, the lowest values were observed in Saint John, consistent with a small city and thus low emissions of gaseous precursors. Shipping emissions in the summer contributed partially to EC concentrations at the coastal sites in Halifax and Burnaby South. The sum of the measured five major components accounted for 51.9%-65.9% of gravimetric $PM_{2.5}$ mass concentrations across Canada. In general, OC contributed most to $PM_{2.5}$, followed by SO_4^{2-} and NO_3^-, while EC and NH_4^+ comprised a small fraction of $PM_{2.5}$. The non-monitored chemical components, such as crustal materials, trace oxidized metals, particle bound water, and other elements in organic matter, totally accounted for about one third of the gravimetric $PM_{2.5}$ mass concentrations, and thus should be measured through scoping studies, if not worth for long-term monitoring, in order to gain a complete picture of $PM_{2.5}$ pollution.

In Atlantic Canada, the highest monthly mean concentrations of the five chemical components were mostly observed in July except for higher monthly concentrations of NO_3^- in January. In western Canada monthly peaks were mostly in January except for SO_4^{2-} which peaked in the summer in Burnaby South. In southeastern Canada, some consistent patterns were observed, such as the highest seasonal SO_4^{2-} concentrations in summer and NO_3^- concentrations in winter, and NH_4^+ peaks in both summer and winter. However, seasonal patterns of OC and EC were different between these southeastern sites, e.g., the highest OC and EC concentrations were observed in summer in Toronto but in winter in Montreal, while the highest OC concentration was in summer but slightly higher EC concentration was observed in winter in Ottawa. The seasonal patterns at the two rural sites roughly followed those at their respective paired urban sites with the exception of absence of the winter peak for OC and EC in Saint Anicet.

Although the seven urban sites studied are located in different regions/airsheds of Canada, air monitoring sites are currently absent in other regions (e.g., central and northern Canada). Future data analysis should include additional sites and longer data records, and combine with modeling studies to identify hotspots of aerosol pollution, assess its potential health impacts, evaluate the effectiveness of existing emission control policies, and provide scientific evidence for developing future emission control strategies.

Appendix A. Supplementary data: Supplementary data to this article can be found online.

Declaration of Competing Interest

The authors declare that they have no conflict of interest.

Acknowledgements

We greatly appreciate all the personnel of the NAPS agencies who operate the sites across Canada, collect 24-hr field samples, continuous data measurements and their QA/QC verification prior to dissemination. The authors would like to acknowledge the staff of the Analysis and Air Quality (Air Quality Research Division) in Ottawa for the laboratory chemical analyses and the QA/QC verification of these data used in the present study. Huanbo Wang was supported by the China Scholarship Council for one year as a visiting fellow at Environment and Climate Change Canada.

Supplementary materials

Supplementary material associated with this article can be found, in the online version, at doi:10.1016/j.jes.2020.09.035.

REFERENCE

Bahadur, R., Feng, Y., Russell, L.M., Ramanathan, V., 2011. Impact of California's air pollution laws on black carbon and their implications for direct radiative forcing. Atmos. Environ. 45, 1162–1167.

Bahadur, R., Praveen, P.S., Xu, Y.Y., Ramanathan, V., 2012. Solar absorption by elemental and brown carbon determined from spectral observations. Proc. Natl. Acad. Sci. USA 109, 17366–17371.

Bari, M.A., Kindzierski, W.B., 2016. Eight-year (2007-2014) trends in ambient fine particulate matter ($PM_{2.5}$) and its chemical components in the Capital Region of Alberta, Canada. Environ. Int. 91, 122–132.

Bhattarai, H., Saikawa, E., Wan, X., Zhu, H.X., Ram, K., Gao, S.P., et al., 2019. Levoglucosan as a tracer of biomass burning: Recent progress and perspectives. Atmos. Res. 220, 20–33.

Blanchard, C.L., Hidy, G.M., Shaw, S., Baumann, K., Edgerton, E.S., 2016. Effects of emission reductions on organic aerosol in the southeastern United States. Atmos. Chem. Phys. 16, 215–238.

Blanchard, C.L., Tanenbaum, S., Hidy, G.M., 2013. Source attribution of air pollutant concentrations and trends in the southeastern aerosol research and characterization (SEARCH) network. Environ. Sci. Technol. 47, 13536–13545.

Chan, E.A.W., Gantt, B., Mcdow, S., 2018. The reduction of summer sulfate and switch from summertime to wintertime $PM_{2.5}$ concentration maxima in the United States. Atmos. Environ. 175, 25–32.

Cheng, Z., Luo, L., Wang, S.X., Wang, Y.G., Sharma, S., Shimadera, H., et al., 2016. Status and characteristics of ambient $PM_{2.5}$ pollution in global megacities. Environ. Int. 89-90, 212–221.

Chow, J.C., Watson, J.G., Chen, L.A., Chang, M.O., Robinson, N.F., Trimble, D., et al., 2007. The IMPROVE-A temperature protocol for thermal/optical carbon analysis: maintaining consistency with a long-term database. J. Air Waste Manage 57, 1014–1023.

Chow, J.C., Watson, J.G., Lu, Z.Q., Lowenthal, D.H., Frazier, C.A., Solomon, P.A., et al., 1996. Descriptive analysis of $PM_{2.5}$ and PM_{10} at regionally representative locations during SJVAQS/AUSPEX. Atmos. Environ. 30, 2079–2112.

Chu, S.H., 2004. $PM_{2.5}$ episodes as observed in the speciation trends network. Atmos. Environ. 38, 5237–5246.

Dabek-Zlotorzynska, E., Celo, V., Ding, L.Y., Herod, D., Jeong, C.H., Evans, G., et al., 2019. Characteristics and sources of $PM_{2.5}$ and reactive gases near roadways in two metropolitan areas in Canada. Atmos. Environ. 218, 116980.

Dabek-Zlotorzynska, E., Dann, T.F., Martinelango, P.K., Celo, V., Brook, J.R., Mathieu, D., et al., 2011. Canadian national air pollution surveillance (NAPS) $PM_{2.5}$ speciation program: methodology and $PM_{2.5}$ chemical composition for the years 2003-2008. Atmos. Environ. 45, 673–686.

Ge, X.L., Zhang, Q., Sun, Y.L., Ruehl, C.R., Setyan, A., 2012. Effect of aqueous-phase processing on aerosol chemistry and size

distributions in Fresno, California, during wintertime. Environ. Chem. 9, 221–235.
Gibson, M.D., Pierce, J.R., Waugh, D., Kuchta, J.S., Chisholm, L., Duck, T.J., et al., 2013. Identifying the sources driving observed $PM_{2.5}$ temporal variability over Halifax, Nova Scotia, during BORTAS-B. Atmos. Chem. Phys. 13, 7199–7213.
Hamburger, T., McMeeking, G., Minikin, A., Birmili, W., Dall'Osto, M., O'Dowd, C., et al., 2011. Overview of the synoptic and pollution situation over Europe during the EUCAARI-LONGREX field campaign. Atmos. Chem. Phys. 11, 1065–1082.
Hand, J.L., Schichtel, B.A., Malm, W.C., Frank, N.H., 2013. Spatial and Temporal Trends in $PM_{2.5}$ Organic and Elemental Carbon across the United States. Adv. Meteorol, 367674.
Hand, J.L., Schichtel, B.A., Malm, W.C., Pitchford, M., Frank, N.H., 2014. Spatial and seasonal patterns in urban influence on regional concentrations of speciated aerosols across the United States. J. Geophys. Res-Atmos. 119, 12832–12849.
Hand, J.L., Schichtel, B.A., Pitchford, M., Malm, W.C., Frank, N.H., 2012. Seasonal composition of remote and urban fine particulate matter in the United States. J. Geophys. Res-Atmos. 117, D05209.
Hansen, D.A., Edgerton, E.S., Hartsell, B.E., Jansen, J.J., Kandasamy, N., Hidy, G.M., et al., 2003. The southeastern aerosol research and characterization study: Part 1-overview. J. Air Waste Manage. 53, 1460–1471.
Healy, R.M., Sofowote, U., Su, Y., Debosz, J., Noble, M., Jeong, C.H., et al., 2017. Ambient measurements and source apportionment of fossil fuel and biomass burning black carbon in Ontario. Atmos. Environ. 161, 34–47.
Hidy, G.M., Blanchard, C.L., Baumann, K., Edgerton, E., Tanenbaum, S., Shaw, S., et al., 2014. Chemical climatology of the southeastern United States, 1999-2013. Atmos. Chem. Phys. 14, 11893–11914.
Hvidtfeldt, U.A., Geels, C., Sorensen, M., Ketzel, M., Khan, J., Tjonneland, A., et al., 2019. Long-term residential exposure to $PM_{2.5}$ constituents and mortality in a Danish cohort. Environ. Int. 133.
Jeong, C.-H., Traub, A., Huang, A., Hilker, N., Wang, J.M., Herod, D., et al., 2020. Long-term analysis of $PM_{2.5}$ from 2004 to 2017 in Toronto: Composition, sources, and oxidative potential. Environ. Pollut. 263, 114652.
Jeong, C.H., Herod, D., Dabek-Zlotorzynska, E., Ding, L.Y., McGuire, M.L., Evans, G., 2013. Identification of the sources and geographic origins of black carbon using factor analysis at paired rural and urban sites. Environ. Sci. Technol. 47, 8462–8470.
Jeong, C.H., Wang, J.M., Hilker, N., Debosz, J., Sofowote, U., Su, Y.S., et al., 2019. Temporal and spatial variability of traffic-related $PM_{2.5}$ sources: Comparison of exhaust and non-exhaust emissions. Atmos. Environ. 198, 55–69.
Malm, W.C., Schichtel, B.A., Hand, J.L., Collett, J.L., 2017. Concurrent Temporal and spatial trends in sulfate and organic mass concentrations measured in the IMPROVE monitoring program. J. Geophys. Res-Atmos. 122, 10341–10355.
Masiol, M., Benetello, F., Harrison, R.M., Formenton, G., De Gaspari, F., Pavoni, B., 2015. Spatial, seasonal trends and transboundary transport of $PM_{2.5}$ inorganic ions in the Veneto region (Northeastern Italy). Atmos. Environ. 117, 19–31.
Masiol, M., Squizzato, S., Rich, D.Q., Hopke, P.K., 2019. Long-term trends (2005-2016) of source apportioned $PM_{2.5}$ across New York State. Atmos Environ 201, 110–120.
McClure, C.D., Jaffe, D.A., 2018. US particulate matter air quality improves except in wildfire-prone areas. Proc. Natl. Acad. Sci. USA 115, 7901–7906.
Myrick, R.H., Sakiyama, S.K., Angle, R.P., Sandhu, H.S., 1994. Seasonal mixing heights and inversions at Edmonton, Alberta. Atmos. Environ. 28, 723–729.
Qiao, B.Q., Chen, Y., Tian, M., Wang, H.B., Yang, F.M., Shi, G.M., et al., 2019. Characterization of water soluble inorganic ions and their evolution processes during $PM_{2.5}$ pollution episodes in a small city in southwest China. Sci. Total. Environ. 650, 2605–2613.
Reid, H., Aherne, J., 2016. Staggering reductions in atmospheric nitrogen dioxide across Canada in response to legislated transportation emissions reductions. Atmos. Environ. 146, 252–260.
Ricciardelli, I., Bacco, D., Rinaldi, M., Bonafe, G., Scotto, F., Trentini, A., et al., 2017. A three-year investigation of daily $PM_{2.5}$ main chemical components in four sites: the routine measurement program of the Supersito Project (Po Valley, Italy). Atmos. Environ. 152, 418–430.
Ridley, D.A., Heald, C.L., Ridley, K.J., Kroll, J.H., 2018. Causes and consequences of decreasing atmospheric organic aerosol in the United States. Proc. Natl. Acad. Sci. USA 115, 290–295.
Salameh, D., Detournay, A., Pey, J., Perez, N., Liguori, F., Saraga, D., et al., 2015. $PM_{2.5}$ chemical composition in five European Mediterranean cities: A 1-year study. Atmos. Res. 155, 102–117.
Schichtel, B.A., Malm, W.C., Bench, G., Fallon, S., McDade, C.E., Chow, J.C., et al., 2008. Fossil and contemporary fine particulate carbon fractions at 12 rural and urban sites in the United States. J. Geophys. Res-Atmos. 113.
Shah, V., Jaegle, L., Thornton, J.A., Lopez-Hilfiker, F.D., Lee, B.H., Schroder, J.C., et al., 2018. Chemical feedbacks weaken the wintertime response of particulate sulfate and nitrate to emissions reductions over the eastern United States. Proc. Natl. Acad. Sci. USA 115, 8110–8115.
Sofowote, U.M., Su, Y.S., Dabek-Zlotorzynska, E., Rastogi, A.K., Brook, J., Hopke, P.K., 2015a. Constraining the factor analytical solutions obtained from multiple-year receptor modeling of ambient $PM_{2.5}$ data from five speciation sites in Ontario, Canada. Atmos. Environ. 108, 151–157.
Sofowote, U.M., Su, Y.S., Dabek-Zlotorzynska, E., Rastogi, A.K., Brook, J., Hopke, P.K., 2015b. Sources and temporal variations of constrained PMF factors obtained from multiple-year receptor modeling of ambient $PM_{2.5}$ data from five speciation sites in Ontario, Canada. Atmos. Environ. 108, 140–150.
Solomon, P.A., Crumpler, D., Flanagan, J.B., Jayanty, R.K.M., Rickman, E.E., McDade, C.E., 2014. US National $PM_{2.5}$ chemical speciation monitoring networks-CSN and IMPROVE: description of networks. J. Air Waste Manage. 64, 1410–1438.
Squizzato, S., Masiol, M., Rich, D.Q., Hopke, P.K., 2018. $PM_{2.5}$ and gaseous pollutants in New York State during 2005-2016: Spatial variability, temporal trends, and economic influences. Atmos. Environ. 183, 209–224.
Thurston, G.D., Ito, K., Lall, R., 2011. A source apportionment of U.S. fine particulate matter air pollution. Atmos. Environ. 45, 3924–3936.
Tian, M., Wang, H.B., Chen, Y., Zhang, L.M., Shi, G.M., Liu, Y., et al., 2017. Highly time-resolved characterization of water-soluble inorganic ions in $PM_{2.5}$ in a humid and acidic mega city in Sichuan Basin, China. Sci. Total Environ. 580, 224–234.
Wang, H.B., Shi, G.M., Tian, M., Zhang, L.M., Chen, Y., Yang, F.M., et al., 2017. Aerosol optical properties and chemical composition apportionment in Sichuan Basin, China. Sci. Total Environ. 577, 245–257.
Wang, H.B., Tian, M., Chen, Y., Shi, G.M., Liu, Y., Yang, F.M., 2018. Seasonal characteristics, formation mechanisms and source origins of $PM_{2.5}$ in two megacities in Sichuan Basin, China. Atmos. Chem. Phys. 18, 865–881.
Wang, H.B., Zhang, L.M., Huo, T.T., Wang, B., Yang, F.M., Chen, Y., et al., 2020. Application of parallel factor analysis model to decompose excitation-emission matrix fluorescence spectra for characterizing sources of water-soluble brown carbon in $PM_{2.5}$. Atmos. Environ. 223.
Wang, X., Heald, C.L., Ridley, D.A., Schwarz, J.P., Spackman, J.R.,

Perring, A.E., et al., 2014. Exploiting simultaneous observational constraints on mass and absorption to estimate the global direct radiative forcing of black carbon and brown carbon. Atmos. Chem. Phys. 14, 10989–11010.
Wiacek, A., Li, L., Tobin, K., Mitchell, M., 2018. Characterization of trace gas emissions at an intermediate port. Atmos. Chem. Phys. 18, 13787–13812.
Xin, J.Y., Wang, Y.S., Pan, Y.P., Ji, D.S., Liu, Z.R., Wen, T.X., et al., 2015. The campaign on atmospheric aerosol research network of China care-China. B. Am. Meteorol. Soc. 96, 1137–1155.
Zhai, X.X., Mulholland, J.A., Russell, A.G., Holmes, H.A., 2017. Spatial and temporal source apportionment of $PM_{2.5}$ in Georgia, 2002 to 2013. Atmos. Environ. 161, 112–121.
Zhang, Y., Huang, W., Cai, T.Q., Fang, D.Q., Wang, Y.Q., Song, J., et al., 2016. Concentrations and chemical compositions of fine particles ($PM_{2.5}$) during haze and non-haze days in Beijing. Atmos. Res. 174, 62–69.
Zheng, G.J., Duan, F.K., Su, H., Ma, Y.L., Cheng, Y., Zheng, B., et al., 2015. Exploring the severe winter haze in Beijing: the impact of synoptic weather, regional transport and heterogeneous reactions. Atmos. Chem. Phys. 15, 2969–2983.